

## Article

# Corrosion Inhibition of Aluminum in Acidic Solution by *Ilex paraguariensis* (Yerba Mate) Extract as a Green Inhibitor

Claudia M. Méndez <sup>1,2,\*</sup> , Claudio A. Gervasi <sup>3,4</sup>, Gonzalo Pozzi <sup>1</sup> and Alicia E. Ares <sup>1,2,\*</sup> 

<sup>1</sup> Programa de Materiales y Fisicoquímica, Facultad de Ciencias Exactas, Químicas y Naturales, Universidad Nacional de Misiones, Félix de Azara 1552, Posadas 3300, Argentina

<sup>2</sup> Instituto de Materiales de Misiones—Consejo Nacional de Investigaciones Científicas y Técnicas, Facultad de Ciencias Exactas, Químicas y Naturales, Universidad Nacional de Misiones, Félix de Azara 1552, Posadas 3300, Argentina

<sup>3</sup> Instituto de Investigaciones Fisicoquímicas Teóricas y Aplicadas—Consejo Nacional de Investigaciones Científicas y Técnicas, Facultad de Ciencias Exactas, Universidad Nacional de La Plata, Diagonal 113 y 64 S/N, La Plata 1900, Argentina

<sup>4</sup> Area Electroquímica, Facultad de Ingeniería, Universidad Nacional de La Plata, Av. 1 750, La Plata 1900, Argentina

\* Correspondence: cmendez@fceqyn.unam.edu.ar (C.M.M.); aares@fceqyn.unam.edu.ar (A.E.A.)

**Abstract:** In the present work, the inhibitory effect of *Ilex paraguariensis* (Yerba Mate) extract on the corrosion of aluminum in 0.1 M HCl solution, in the temperature range of 298–323 K, was studied by using weight loss tests, potentiodynamic polarization measurements and electrochemical impedance spectroscopy (EIS). The extract of *Ilex paraguariensis* exhibits improved inhibitory action as its concentration increases while its performance is maintained despite an increase in temperature. EIS theoretical data according to a suitable proposed equivalent circuit were successfully fitted to the experimental data. The adsorption of organic compounds followed a modified Langmuir isotherm behaviour. Derived thermodynamic parameters indicate the occurrence of both chemical and physical adsorption.

**Keywords:** *Ilex paraguariensis*; green corrosion inhibitor; EIS; adsorption isotherm



**Citation:** Méndez, C.M.; Gervasi, C.A.; Pozzi, G.; Ares, A.E. Corrosion Inhibition of Aluminum in Acidic Solution by *Ilex paraguariensis* (Yerba Mate) Extract as a Green Inhibitor. *Coatings* **2023**, *13*, 434. <https://doi.org/10.3390/coatings13020434>

Academic Editor: Alina Vladescu

Received: 31 January 2023

Revised: 10 February 2023

Accepted: 14 February 2023

Published: 15 February 2023



**Copyright:** © 2023 by the authors. Licensee MDPI, Basel, Switzerland. This article is an open access article distributed under the terms and conditions of the Creative Commons Attribution (CC BY) license (<https://creativecommons.org/licenses/by/4.0/>).

## 1. Introduction

Many industrial processes are closed and need to recirculate fluids. Thus, to reduce costs and reduce the corrosion rate of the materials involved in the construction of industrial plants, it is necessary to use corrosion inhibitors. These inhibitors can be either inorganic, such as chromates, dichromates, and nitrites, or organic. Typical organic inhibitors contain nitrogen, sulfur or oxygen in their molecular structure or as functional groups, or  $\pi$  electrons in their double or triple conjugated bonds [1–3]. The mechanism by which these organic inhibitors act is by adsorption on the surface of the metal. Adsorption can take place through (1) electrostatic attraction of the charged metal and the charged molecule of the inhibitor, (2) attraction of the vacant orbitals of the metal interacting with the free electrons of the heteroatom (N, S or O), (3) interaction of the  $\pi$  electrons of the aromatic rings with the metal, and, when possible, (4) a combination of the three mentioned processes. Since many organic inhibitors are toxic and expensive, researchers are looking for products that are more environmentally friendly, i.e., the so-called green corrosion inhibitors [4–10].

Molecules obtained from natural compounds, extracted for example from plant tissues, are receiving definite preference as corrosion inhibitors, because they are easy to apply, safe, biodegradable, inexpensive and easily extractable from renewable sources [11,12]. Thus, different substances of natural origin have been evaluated as inhibitors of the corrosion of different metals in acidic media. These include *Rollinia occidentalis* extracts for carbon steel [13], *Brassica campestris* extract for steel [14], *Musa paradisiaca* skin extract for mild steel [15], and *Hena* extract for iron [16]. Several substances have also been evaluated as

inhibitors of the corrosion of aluminum in an acidic medium. These include: essential oil of *Eucalyptus camaldulensis* and *Myrtus Communis* [17], *Camellia sinensis* extract [18], *Trigonellafoenum-graecum* L Seeds extract [19], pectin from the peel of citrus fruits [20], *Artemisia Herba Alba* essential oil [21], *Dryopteris cochleata* leaf extract [22], Shatavari (*Asparagus Racemosus*) [23], Azwain seed extract [24], *Ipomoea involvcrata* extract [25], and *Terminalia ivorensis* extract [26]. The abundance, renewal and biological elimination of these inhibitors are key to their implementation [7,11–27].

*Ilex paraguariensis* is a tree species whose extracts have not yet been thoroughly explored as corrosion inhibitors. This tree grows in South America, occupying an area of 540,000 km<sup>2</sup> distributed in Argentina, Brazil and Paraguay [28]. Its leaves and branches are processed to obtain three final products: elaborated yerba mate, tea bags and soluble mate, but after its processing, a 3% is lost as unused waste, in the form of small pieces of sticks and dust. This organic material can be reused advantageously as a raw material to obtain organic inhibitors that additionally reduce environmental discharge. Before becoming a soluble product, *Ilex paraguariensis* undergoes a process known as spray drying, in which a liquid (a solution, emulsion or suspension) is atomized into a stream of hot gas (usually air or an inert gas such as nitrogen) to convert it into a powder product. This guarantees the microbiological stability of the product, and reduces the probability of chemical and biochemical degradation, reducing the cost of storage and transport [29]. The two most important compounds in aqueous extracts are polyphenols (42% chlorogenic acid) and xanthines (caffeine 8%, theobromine 2% and theophylline 1%), followed by purine alkaloids (4,5-dicaphoxyquinic acid 11%, 3,4-dicaffeoylquinic acid, 3,5-dicaffeoylquinic acid), flavonoids (quercetin, kaempferol, and rutin), amino acids, and, to a lesser extent, saponins, minerals (P, Fe, and Ca), and vitamins (C, B1, and B2) [30,31] (Figure 1). Under spray-drying conditions, the loss of polyphenolic compounds is negligible [29]. Based on the aspects described above, the objective of this work is to study *Ilex paraguariensis* extract as a possible green inhibitor of aluminum corrosion in HCl solution, elucidate the mechanisms of protection and the effects of temperature and concentration on its performance. Accordingly, the inhibited surface is characterized by using weight loss tests, potentiodynamic polarization measurements and electrochemical impedance spectroscopy (EIS).

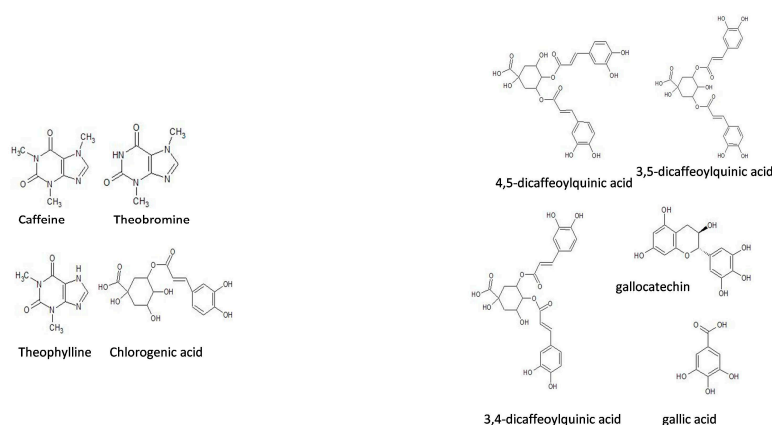


**Figure 1.** Some of the chemical structures of *Ilex paraguariensis* components.

## 2. Materials and Methods

### 2.1. Preparation of Aluminum Samples and Solutions

Aluminum, whose composition (%wt) was completed with Si (0.05%), Fe (0.06%), and Zn (0.01%), was used as test material. Samples of 1 cm<sup>2</sup> were cut to assemble the working electrodes to be used in electrochemical measurements, and samples of 5–6 cm<sup>2</sup> were used for weight loss tests. The samples were ground with SiC paper with granulometries of # 500, # 600, # 1000 and # 1200, washed and treated with water immersion ultrasound and finally air dried. Solutions of HCl 0.1 M, of analytical grade Cicarelli, were prepared without and with *Ilex paraguariensis* extract in concentrations of 0.064, 0.124 and

0.248 g/L. The composition (% w/w) of the *Ilex paraguariensis* extract was mainly polyphenols (chlorogenic acid 42%) and xanthenes (caffeine 8%, theobromine 2% and theophylline 1%), 1.3% glucose, 7.4% sucrose, the rest by purine alkaloids (4,5-dicaphoxyquinic acid 11%, 3,4-dicaffeoylquinic acid, 3,5-dicaffeoylquinic acid), flavonoids, amino acids, and, to a lesser extent, saponins, minerals and vitamins.

## 2.2. Weight Loss Measurements

The aluminum samples were immersed in four closed cups containing a solution of 0.1 M HCl, three with concentrations of 0.064, 0.124 and 0.248 g L<sup>-1</sup> of *Ilex paraguariensis* and the fourth cup without *Ilex paraguariensis*. Experiments were performed at 298, 308, 315 and 323 K by immersing the beakers in a thermostatic bath. In all four cups, the samples remained submerged for 48 h. After this period, the specimens were removed from the thermostat, washed with distilled water, subjected to ultrasonic cleaning by using a laboratory sonicator Arcano, and finally air-dried. Then, they were weighed, with an analytical balance Mettler model H72, before and after the test, and the weight loss recorded. The efficiency of *Ilex paraguariensis* as an inhibitor was calculated by Equation (1):

$$\eta_w \% = \frac{C_R^0 - C_R^i}{C_R^0} \times 100 \quad (1)$$

where  $C_R^0$  is the corrosion rate (g cm<sup>-2</sup> h<sup>-1</sup>) of the aluminum in the absence of the inhibitor and  $C_R^i$  is the corrosion rate (g cm<sup>-2</sup> h<sup>-1</sup>) of the aluminum in the presence of the inhibitor. Corrosion rate as per weight loss was calculated according to Equation (2)

$$C_R = \frac{\Delta W}{S \times t} \quad (2)$$

where  $\Delta W$  is the average weight loss,  $S$  the total area of the specimen, and  $t$  is the immersion, time.

## 2.3. Electrochemical Measurements

A three-electrode cell with a saturated calomel electrode (SCE) as reference electrode, a platinum counter electrode, and the aluminum working electrode was used for the electrochemical measurements. All potentials mentioned in this work are expressed vs. the SCE. Experiments were performed at 298, 308, 315 and 323 K, in the absence or in the presence of *Ilex paraguariensis* at concentrations of 0.064, 0.124 and 0.248 g L<sup>-1</sup>. A Gamry Reference 600<sup>®</sup> potentiostat was used.

### 2.3.1. Potentiodynamic Polarization (PP) Measurements

The potentiodynamic polarization curves were recorded after keeping the samples for 30 min at the open circuit potential ( $E_{op}$ ) that was required for them to reach a pseudo-stationary state. Then, the electrode potential was varied linearly, at a sweep speed of 0.16 mV s<sup>-1</sup>, from -500 mV with respect to the open circuit potential ( $E_{op}$ ) to ca. +200 mV (vs  $E_{op}$ ).

Polarization data were treated by using the Gamry Echem data-analysis software Analyst<sup>™</sup>. Thus, corrosion potentials ( $E_{corr}$ ), corrosion current densities ( $I_{corr}$ ), anodic and cathodic Tafel slopes ( $\beta_a$ ,  $\beta_c$ ), and polarization resistances ( $R_p$ ) for each experiment were determined. In turn, these data were used to determine the inhibition efficiency ( $\eta_I$ %), calculated from the values obtained for  $I_{corr}$  with Equation (3):

$$\eta_I \% = \frac{I_{corr}^0 - I_{corr}^i}{I_{corr}^0} \times 100 \quad (3)$$

where  $I_{corr}^0$  is the corrosion current in the absence of the inhibitor and  $I_{corr}^i$  is the corresponding corrosion current in the presence of the inhibitor.

### 2.3.2. Electrochemical Impedance Spectroscopy

EIS measurements were carried out in the frequency range of 0.010 Hz–100 kHz, by applying 10 mV (peak to peak) amplitude, alternating potential signals, after an initial conditioning time of 30 min at the open circuit potential. The charge resistance ( $R_{ct}$ ) for the corrosion reaction was derived from a data fitting procedure by using a theoretical impedance function, as described below. Accordingly, the efficiency of *Ilex paraguariensis* as an inhibitor was then determined through Equation (4):

$$\eta_R\% = \frac{R_{ct}^i - R_{ct}^0}{R_{ct}^i} \times 100 \quad (4)$$

where  $R_{ct}^0$  is the charge transfer resistance in the absence of the inhibitor, and  $R_{ct}^i$  is the charge transfer resistance in the presence of the inhibitor.

### 2.4. Surface Analysis

Surface imaging was performed on samples that were immersed in 0.1 M HCl for 48 h at a temperature of 308 K. One of the samples was in the absence of *Ilex paraguariensis*, and the other in the presence of *Ilex paraguariensis* at a concentration of 0.248 g L<sup>-1</sup>. The analysis was performed by metallographic optical microscopy with an Arcane<sup>®</sup> metallographic microscope and by scanning electron microscopy (SEM) with a SUPRA 40, Carl Zeiss NTS.

## 3. Results and Discussion

### 3.1. Weight Loss Measurements

Table 1 shows the results of weight loss measurements for aluminum corrosion in 0.1 M HCl solution in the presence and in the absence of *Ilex paraguariensis* extract at different concentrations and temperatures. The use of *Ilex paraguariensis* led to a decrease in the corrosion rate ( $C_R$ ). This decrease was larger as the amount of inhibitor in the solution increased (Figure 2). This is expressed in terms of the inhibition efficiency ( $\eta_w\%$ ) shown in Table 1 and could be due to the adsorption of organic molecules from the extract on the aluminum surface. Thus, an increase in the surface coverage is directly related to a decrease in the extent of the corrosive attack. Previous reports have shown that the adsorption of heterocyclic compounds occurs with aromatic rings mostly oriented perpendicular to the metal surface at low concentration. On the other hand, at a high inhibitor concentration, adsorbate molecules are reoriented according to a parallel mode, covering a larger surface [32].

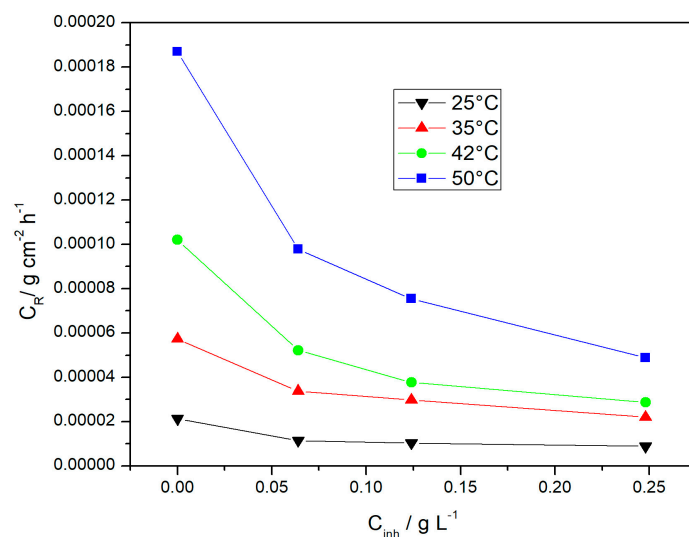


**Figure 2.** Corrosion rate ( $C_R$ ) of aluminum in 0.1 M HCl containing various concentrations of *Ilex paraguariensis* extract ( $C_{inh}$ ) at different temperatures.

**Table 1.** Weight loss of aluminum in a 0.1 M HCl solution, at different temperatures and concentrations of *Ilex paraguariensis* as an inhibitor, after 48 h immersion time.

Temperature (K)	Concentration (g L <sup>-1</sup> )	C <sub>R</sub> × 10 <sup>5</sup> (g cm <sup>-2</sup> h <sup>-1</sup> )	η <sub>w</sub> (%)
298	0	2.13	–
	0.064	1.14	46
	0.124	1.03	50
	0.248	0.89	54
308	0	5.73	–
	0.064	3.38	41
	0.124	2.97	46
	0.248	2.20	57
315	0	10.2	–
	0.064	5.22	49
	0.124	3.77	62
	0.248	2.87	69
323	0	18.7	–
	0.064	9.78	47
	0.124	7.54	58
	0.248	4.89	71

As the temperature increases, corrosion rates increase both in the blank solution and in the solutions containing different concentrations of the inhibitor. Worthy of note, for the largest tested inhibitor concentration, the protection efficiency also increases as the temperature increases. *Ilex paraguariensis* exhibits better performance at high temperatures.

### 3.2. Effect of Temperature

The apparent activation energy for aluminum corrosion in acidic medium, in the presence and in the absence of the inhibitor, was determined by the Arrhenius Equation (5):

$$\log C_R = \frac{-E_a}{2.303 RT} + \log A \quad (5)$$

where C<sub>R</sub> is the corrosion rate, E<sub>a</sub> is the apparent activation energy, T is the absolute temperature, R is the ideal gas constant (8.314 J K<sup>-1</sup> mol<sup>-1</sup>), and A is the frequency factor.

Figure 3 shows log C<sub>R</sub> vs. 1/T data, whose linear regression yields the corresponding parameters, namely, slope, intercept and correlation coefficient for each straight line according to the inhibitor concentration. Linear regression coefficients are close to 0.99, indicating that aluminum corrosion in 0.1 M HCl solution can be elucidated with reasonable certainty by using the kinetic model. The activation energy shown in Table 2 was derived from these regression parameters.

**Table 2.** Thermodynamic properties E<sub>a</sub>, ΔH<sub>a</sub><sup>\*</sup> and ΔS<sub>a</sub><sup>\*</sup> (see definitions in text) for aluminum in 0.1 M HCl blank solution and in the blank solution with different concentrations of *Ilex paraguariensis*.

C <sub>inh</sub> (g L <sup>-1</sup> )	E <sub>a</sub> (kJ mol <sup>-1</sup> K <sup>-1</sup> )	ΔH <sub>a</sub> <sup>*</sup> (kJ mol <sup>-1</sup> )	ΔS <sub>a</sub> <sup>*</sup> (J mol <sup>-1</sup> K <sup>-1</sup> )
0	69.52	66.95	–115.18
0.064	67.88	65.30	–125.61
0.124	61.44	58.86	–148.01
0.248	53.30	50.72	–176.61

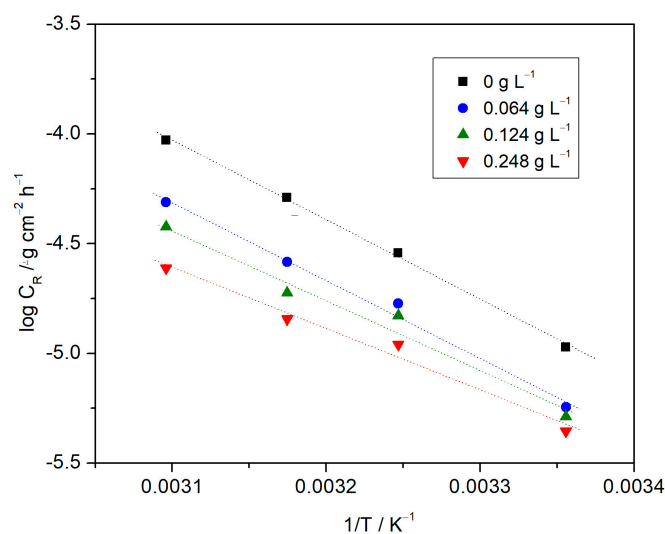


**Figure 3.** Arrhenius plots for the corrosion rate of aluminum in a 0.1 M HCl solution, in the presence and absence of *Ilex paraguariensis* extract.

$E_a$  values decrease with the concentration of *Ilex paraguariensis*, as can be observed from the results in Table 1, while inhibition efficiency increased slightly or remained constant as the temperature increased. These values are similar to those involving chemical reactions in electrolyte solutions [33]. Souza et al. [34] found that, for carbon steel corrosion in 1 M HCl, both in the presence and in the absence of *Ilex paraguariensis* extracts, the  $E_a$  value obtained in the blank solution was  $38.7 \text{ kJ mol}^{-1}$ , and in the presence of *Ilex paraguariensis*, the value was  $37.3 \text{ kJ mol}^{-1}$ . These authors also found that the inhibition efficiency remained almost constant at various temperatures, and concluded that this may result from chemisorption of the inhibitor on the surface of the steel, product of the charge transfer between the inhibitor molecules of *Ilex paraguariensis* present and the surface of the metal. The same fact has been previously observed when caffeic acid acts as corrosion inhibitor for mild steel in 0.1 M  $\text{H}_2\text{SO}_4$ , since the activation energy values in the presence and in the absence of the inhibitor ranged from  $59.74 \text{ kJ mol}^{-1}$  to  $63.95 \text{ kJ mol}^{-1}$ , respectively [35]. In general, it is accepted that a decrease in the activation energy with an increase in the inhibitor concentration points to a specific adsorption interaction or chemisorption processes [36]. This might also result from the nature of the adsorption mode changing from physical adsorption at low temperatures to chemisorption as the temperature increases. Noor et al. [37] suggested that the increase in temperature may produce chemical changes in the inhibitor molecules, increasing electron density in the molecule's adsorption centers, that is related to improved inhibition efficiency [38].

To calculate enthalpy change values ( $\Delta H_a^*$ ) and activation entropy change ( $\Delta S_a^*$ ), we used Equation (6):

$$\log \frac{C_R}{T} = \left[ \log \frac{k_b}{h} + \left( \frac{\Delta S_a^*}{2.303R} \right) \right] - \left( \frac{\Delta H_a^*}{2.303RT} \right) \quad (6)$$

where  $k_b$  is the Boltzmann constant and  $h$  is the Planck constant.

The resulting values for  $\Delta H_a^*$  and  $\Delta S_a^*$  are presented in Table 2. The positive value in the enthalpic change for the activation complex in the transition state ( $\Delta H_a^*$ ) reflects the endothermic nature of the aluminum corrosion process. The corresponding entropic change ( $\Delta S_a^*$ ) values decreased with the increase in *Ilex paraguariensis* concentration, indicating that the process becomes more orderly as the inhibitor covers the surface of the metal, in addition to the fact that the adsorption mode is rather slow and the rate determining step is one of adsorption rather than desorption.

### 3.3. Potentiodynamic Polarization Measurement

The potentiodynamic polarization curves of aluminum in 0.1 M HCl solution recorded in the presence and in the absence of *Ilex paraguariensis* as a corrosion inhibitor at different temperatures are shown in Figure 4.

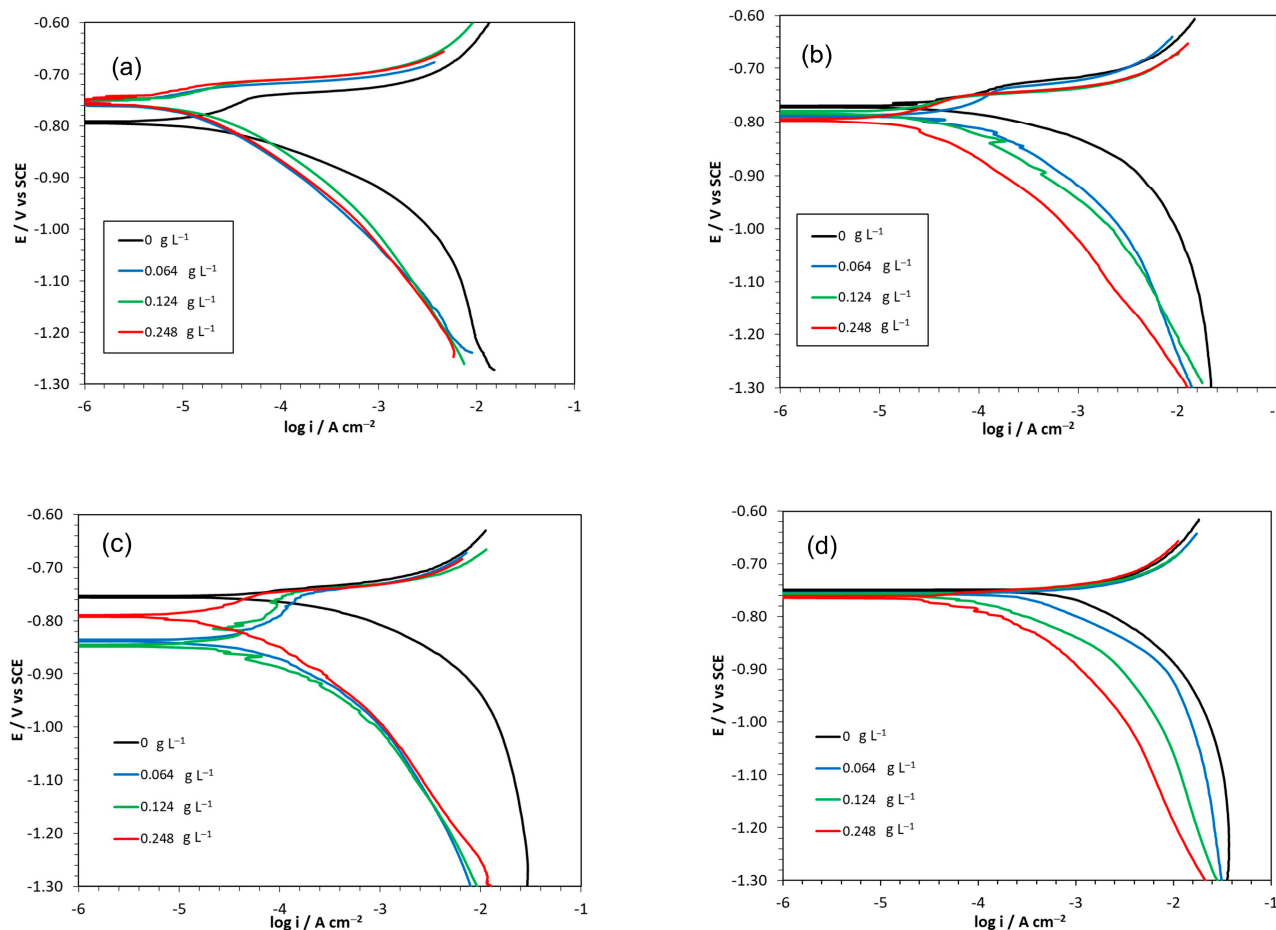


**Figure 4.** Effect of *Ilex paraguariensis* concentration on the polarization curves of the aluminum polarization in the blank solution and in inhibited solutions with different inhibitor concentrations at 298 K (a), 308 K (b), 315 K (c) and 323 K (d).

By using the Tafel extrapolation method, the following electrochemical parameters were calculated:  $E_{\text{corr}}$ ,  $I_{\text{corr}}$ , and anodic ( $\beta_a$ ) and cathodic ( $\beta_c$ ) Tafel slopes. These are shown in Table 3, where it can be observed that the corrosion current density decreased with increasing concentration of *Ilex paraguariensis*, reaching a maximum inhibition efficiency of 91%.

The Tafel slopes ( $\beta_a$  and  $\beta_c$ ) did not vary significantly with the increase in *Ilex paraguariensis* concentration (Table 3). Consequently, reaction mechanisms of anodic and cathodic reactions were not altered by the presence of the inhibitor. The potentiodynamic measurements showed that the presence of *Ilex paraguariensis* caused only negligible changes in the Tafel slopes. However, it stands out that the values for the Tafel slopes indicate that both anodic and cathodic reactions are activation-controlled, perhaps with the single exception of the cathodic branch for 323 K. Moreover, no active–passive transition is evident in the anodic branches of the polarization curves. It has been suggested that cathodic Tafel slopes larger than  $180 \text{ mV dec}^{-1}$  might indicate  $\text{H}_2$  evolution occurring on a surface layer covering the aluminum substrate and building a potential energy barrier for the charge carriers.

**Table 3.** Electrochemical parameters obtained from the Tafel curves for aluminum corrosion in HCl 0.1 M in the presence and in the absence of *Ilex paraguariensis* at different concentrations and working temperatures.

Temperature (K)	C <sub>inh</sub> (g L <sup>-1</sup> )	E <sub>corr</sub> (mV vs. SCE)	I <sub>corr</sub> (μA cm <sup>-2</sup> )	β <sub>a</sub> (mV dec <sup>-1</sup> )	-β <sub>c</sub> (mV dec <sup>-1</sup> )	η <sub>I</sub> (%)
298	0	-793.03	23.60	180	80	-
	0.064	-756.28	9.42	100	120	60
	0.124	-810.22	17.9	120	100	44
	0.248	-754.99	7.12	120	80	70
308	0	-770.85	57.4	70	45	-
	0.064	-788.33	41.1	110	75	28
	0.124	-782.31	26.1	70	80	54
	0.248	-796.11	20.2	100	100	65
315	0	-754.71	297	60	150	-
	0.064	-837.19	44.8	120	90	85
	0.124	-846.81	36.9	120	70	88
	0.248	-791.08	28.2	120	120	91
323	0	-751.64	2320	90	400	-
	0.064	-757.60	1750	70	400	25
	0.124	-759.04	1320	70	400	43
	0.248	-763.83	680	70	400	71

E<sub>corr</sub> did not have a clear tendency to shift towards either more cathodic or more anodic values, except for experiments at 323 K. Thus, we cannot say for certain whether *Ilex paraguariensis* is a cathodic or an anodic inhibitor since the difference between E<sub>corr</sub> with and without *Ilex paraguariensis* did not exceed ±85 mV to define its nature [39]. This behavior can be attributed to a decrease in the dissolution rate of the metal by adsorption of organic compounds or protonated forms on the surface of the metal. Thus, *Ilex paraguariensis* can be described as a mixed-type inhibitor.

As indicated above, only negligible changes in both anodic and cathodic Tafel slopes were recorded according to changes in the inhibitor concentration. Thus, when the single inhibition mechanism is due to a blocking effect of the electroactive area by adsorption with a coverage of 0.5 on cathodic sites and equally 0.5 on anodic sites, then E<sub>corr</sub> remains invariant. This may be the case for condition T = 308 K (Figure 4b). However, E<sub>corr</sub> shifts in the positive direction when the fractional surface coverage of the anodic sites becomes larger than the corresponding coverage of the cathodic sites as for T = 298 K (Figure 4a). Finally, when the opposite is valid, namely larger coverage of the cathodic sites as compared with the coverage of the anodic sites, then E<sub>corr</sub> shifts in the negative direction, as in the case for T = 315 K (Figure 4c). In this scenario, increasing temperatures could promote coverage imbalance favoring the cathodic sites over the anodic sites. The case for T = 323 K was not included in this analysis, since this represents a singularity, as discussed elsewhere in the text.

According to Abd El Haleem et al. [40], when the aluminum is immersed in an inhibitor-free 2 M HCl solution, during the first 10 min of immersion, the oxide barrier layer results completely dissolved. This is due to formation of a soluble complex ion between aluminum and chloride ions of the solution; see the reaction that follows [23]:



The destruction of an outer layer, if present, may require longer times, which additionally depends on the inhibitor concentration. Thus, when corrosion potentials shift towards the anodic direction with the addition of an inhibitor is because the destruction of the oxide film is hindered and the capacity of film healing by the adsorbed species is higher. However, E<sub>corr</sub> becomes more cathodic when the protection is not afforded [40]. It has also been stated that the thickness of an external porous layer depends on the temperature.

Moreover, there is an inhibitor concentration limiting value at which the rate of healing of the protective oxide film begins to exceed that of the oxide dissolution, thanks to the effective adsorption of the inhibitor.

### 3.4. Electrochemical Impedance Spectroscopic Measurements

EIS measurements are performed to investigate corrosion inhibition processes at the metal/solution interface, which allows us to gain a deeper insight into the inhibition mechanisms. Figure 5 shows impedance spectra recorded at 308 and 323 K and *Ilex paraguariensis* concentrations. Impedance spectra in Figure S1 show equivalent results recorded at 298 and 315 K.

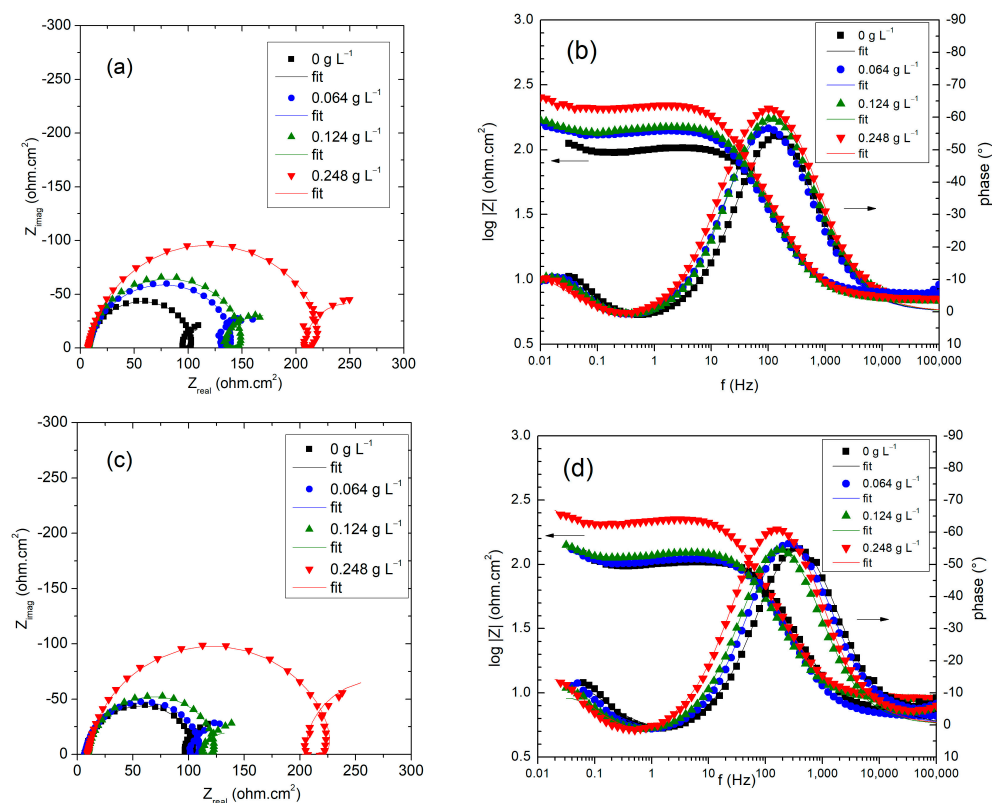


**Figure 5.** Nyquist and Bode representations of experimental data and fit results of electrode impedance recorded for the system Al/0.1 M HCl in the absence and in the presence of different concentrations of the inhibitor at 308 K (a,b), and 323 K (c,d).

Both Nyquist and Bode representations of impedance data clearly show relaxation of three distinct interfacial processes that enable us to distinguish three corresponding time constants. A capacitive loop in the high-frequency range is followed by an inductive arc at intermediate frequencies and, finally, a capacitive contribution in the low-frequency range [17,23,41]. These features were understood in terms of a model containing the non-faradic impedance (due to the charging of the double-layer capacitor) in parallel connection with the faradaic impedance related to the electrochemical reactions. In turn, the faradaic impedance contains the charge-transfer resistance  $R_{\text{ct}}$  that is a measure of the aluminum dissolution process, and it was shown to be the element that most accurately correlates with the corrosion rate [42,43]. The proposed theoretical impedance corresponds to the impedance of the equivalent circuit in Figure 6, where  $R_{\text{ct}}$  is given, to a first approximation, by the length of the chord of the capacitive semicircular arc at high frequencies in a Nyquist plot. Dynamic features of the interfacial electrode processes remain unchanged for measurements performed both with and without *Ilex paraguariensis* inhibitor, thus indicating that the same theoretical proposal is applicable in the presence and in the absence of the inhibitor [33]. Capacitances in the system were considered as distributed impedance

elements by using the constant-phase-element CPE definition in Equation (8) [44]. Inductive loops in comparable corrosion studies are frequently reported in the literature [45] and are typically correlated with the relaxation of adsorbed reaction intermediates. The capacitive loop at low frequencies is considered in the model as resulting from an adsorption step of a reactant species.

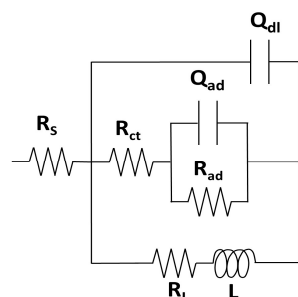


Figure 6. Equivalent circuit used for the impedance-fitting procedure.

The length of the chord of the capacitive loop at high frequencies in Nyquist plots increases according to the *Ilex paraguariensis* content, indicating a stronger action of the inhibitor as its concentration increases. As can be observed in Figure 5, EIS theoretical data from the proposed equivalent circuit (Figure 6) were successfully fitted to the experimental data.

The equivalent circuit in Figure 6 contains the following elements:  $R_s$  is the solution resistance, the constant phase element (CPE)  $Q_{dl}$  represents a distributed impedance element for the double layer capacitor,  $R_{ct}$  is the charge-transfer resistance,  $R_{ad}$  is the adsorption resistance and the constant phase element (CPE)  $Q_{ad}$  represents an adsorption pseudo-capacitance.  $R_L$  and  $L$  represent the Resistor and Inductor of the inductive impedance, respectively. The best-fit values of the parameters from the equivalent circuit are shown in Table 4.

Table 4. Estimates of impedance parameters resulting from a complex non-linear least-squares analysis of the experimental impedance spectra and the corresponding inhibition efficiencies of aluminum in 0.1 M HCl in the presence and in the absence of different concentrations of *Ilex paraguariensis*.

T (K)	Conc (g L <sup>-1</sup> )	Q <sub>dl</sub>		R <sub>ct</sub> (ohm cm <sup>2</sup> )	Q <sub>ad</sub>		R <sub>ad</sub> (ohm cm <sup>2</sup> )	η <sub>R</sub> (%)
		Y <sub>o</sub> (ohm <sup>-1</sup> cm <sup>-2</sup> s <sup>α</sup> )	α		Y <sub>o</sub> (ohm <sup>-1</sup> cm <sup>-2</sup> s <sup>α</sup> )	α		
298	0	6.86 × 10 <sup>-5</sup>	0.90	212.22	1.45 × 10 <sup>-1</sup>	1.00	144.88	0.00
	0.064	8.34 × 10 <sup>-5</sup>	0.86	376.01	1.62 × 10 <sup>-1</sup>	1.00	192.33	43.56
	0.124	6.59 × 10 <sup>-5</sup>	0.89	490.05	*	*	*	56.69
	0.248	8.04 × 10 <sup>-5</sup>	0.89	528.13	*	*	*	59.81
308	0	7.73 × 10 <sup>-5</sup>	0.91	105.00	1.57 × 10 <sup>-1</sup>	1.00	45.57	0.00
	0.064	9.33 × 10 <sup>-5</sup>	0.90	141.05	1.74 × 10 <sup>-1</sup>	0.99	103.17	25.56
	0.124	7.62 × 10 <sup>-5</sup>	0.91	152.15	1.79 × 10 <sup>-1</sup>	1.00	87.33	30.98
	0.248	7.09 × 10 <sup>-5</sup>	0.90	223.25	1.69 × 10 <sup>-1</sup>	1.00	106.70	52.96
315	0	4.99 × 10 <sup>-5</sup>	0.93	86.15	0.82 × 10 <sup>-1</sup>	1.00	59.95	0.00
	0.064	7.78 × 10 <sup>-5</sup>	0.90	86.49	1.83 × 10 <sup>-1</sup>	1.00	34.75	0.39
	0.124	6.77 × 10 <sup>-5</sup>	0.89	167.62	1.38 × 10 <sup>-1</sup>	1.00	276.92	48.60
	0.248	6.22 × 10 <sup>-5</sup>	0.91	187.00	1.29 × 10 <sup>-1</sup>	1.00	78.05	53.93
323	0	3.33 × 10 <sup>-5</sup>	0.91	106.24	0.58 × 10 <sup>-1</sup>	1.00	57.16	0.00
	0.064	4.45 × 10 <sup>-5</sup>	0.91	114.58	0.78 × 10 <sup>-1</sup>	1.00	57.58	7.27
	0.124	4.93 × 10 <sup>-5</sup>	0.91	123.89	1.11 × 10 <sup>-1</sup>	1.00	49.96	14.25
	0.248	4.00 × 10 <sup>-5</sup>	0.91	226.50	0.56 × 10 <sup>-1</sup>	1.00	203.12	53.09

The impedance Z of a CPE can be expressed mathematically, as in Equation (8):

$$Z_{CPE} = Y_0^{-1}(iw)^{-\alpha} \quad (8)$$

where  $Y_0$  and  $\alpha$  are  $Z_{CPE}$  fit parameters,  $w$  is the angular frequency and  $i = \sqrt{-1}$ . Table 4 shows that the  $\alpha$  values for the double layer capacitance exhibit a negligible decrease as inhibitor concentration increases at room temperature but, at higher temperatures, remain invariant [15,33,46]. For the pseudo-capacitance  $\alpha$  values are essentially always equal to 1, indicating a non-distributed capacitance. Moreover,  $Y_0$  values resulting from the fitting procedure for the double layer capacitance are in the order of magnitude expected for the charging of a double-layer capacitor and those values for a pseudo-adsorption step are also typical for a space-charge layer formed by charged adsorbate species.

Based on a comparison between  $\eta$  and the relative coverage (as determined from  $C_{dl}$ ), inhibition can be associated with a geometric blocking effect [47]. For that purpose, the double layer capacitance was calculated from Equation (9):

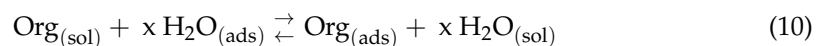
$$C_{dl} = (2\pi f_m R_{ct})^{-1} \quad (9)$$

where  $f_m$  is the frequency at which the imaginary component of the interfacial impedance  $Z''$  exhibits a maximum in the high-frequency region related to the charge-transfer process.

Table 4 shows that, for each considered temperature,  $R_{ct}$  increased with the concentration of *Ilex paraguariensis*, due to the adsorption of organic molecules on the aluminum surface. Adsorption, in turn, blocks the transport of chemical species through the interface, leading to the corrosion inhibition. Considering Equation (8), we observed that the frequency  $f_m$  for the  $Z''$  maximum remained mostly unchanged, as expected for a time constant  $C_{dl} \times R_{ct}$  independent of the electroactive area [40]. On the other hand, unexpected reductions in  $C_{dl}$  values were explained in the literature as the decrease in the local dielectric constant or the increase in the thickness of the electrical double layer. The former case might suggest the substitution of  $H_2O$  molecules (with a higher dielectric constant) by inhibitor molecules (with a lower dielectric constant), leading to the formation of a thin protective film on the electrode surface [48].

### 3.5. Adsorption Isotherm

It is widely accepted that the essential mechanism by which an organic corrosion inhibitor acts on the metal surface is adsorption [49,50]. This phenomenon may be due to the quasi-replacement of water molecules on the metal surface ( $H_2O_{(ads)}$ ) with organic compounds from the solution ( $Org_{(sol)}$ ):



where  $x$  is the ratio of the number of water molecules replaced per inhibitor molecule.

Since more information on the interaction between the inhibitor molecules and the metal surface can be obtained from the study of the adsorption isotherm, we tested the fitting of various adsorption isotherms (such as Langmuir, Temkin and Frumkin) to the data:

$$\text{Langmuir Isotherm : } \frac{C_{inh}}{\theta} = \frac{1}{K_{ads}} + C_{inh} \quad (11)$$

$$\text{Temkin Isotherm : } \log\left(\frac{\theta}{C_{inh}}\right) = \log K_{ads} - g \times \theta \quad (12)$$

$$\text{Frumkin Isotherm : } \log\left(\frac{\theta}{(1-\theta)C_{inh}}\right) = \log K_{ads} + g \times \theta \quad (13)$$

where  $\theta$  is the surface coverage,  $K_{ads}$  is the adsorption equilibrium constant,  $C_{inh}$  is the inhibitor concentration, and  $g$  is the adsorbate interaction parameter. If a Langmuir isotherm fits to the data, it is assumed that there is no interaction between the molecules adsorbed on the surface; if a Temkin isotherm fits to them, it is assumed that there is adsorption in multilayers; and if a Frumkin isotherm represents the suitable fitting function, it is considered that there is some interaction between adsorbates. Through fitting to weight-loss results,

Frumkin and Temkin isotherms were discarded because the obtained  $K_{ads}$  decreased with the increase in temperature, contrasting with the results indicating that, as the temperature increases, increases the inhibitor efficiency.

For the Langmuir isotherm, we contemplated its correction because the slopes of the straight lines obtained were either greater or smaller than 1 for all the temperatures. The considerable deviation from unity may be due to the interactions between the species adsorbed on the surface of the metal. Therefore, it is pertinent to say that adsorption may be more appropriately represented by a modified Langmuir equation, namely, either the isotherm of Villamil et al. [51] or that of El-Awady [52]:

$$\text{Villamil Isotherm : } \frac{C_{inh}}{\theta} = \frac{n}{K_{ads}} + n \times C_{inh} \quad (14)$$

$$\text{El - Awady Isotherm : } \log\left(\frac{\theta}{1-\theta}\right) = \log K' + y \times \log C_{inh} \quad (15)$$

where  $K'$  is a constant related to the equilibrium constant of adsorption process ( $K_{ads}$ ) as

$$K_{ads} = K'^{1/y} \quad (16)$$

In the isotherm of Villamil, the value of “n” is a constant introduced to consider all the factors, ignored the derivation of the isotherm of Langmuir. This occurs when the slope in the Langmuir equation is not 1 and it must then be considered that there is an interaction between the species adsorbed on the surface of the metal [26]. The constant  $y$  in the El-Awady isotherm is the number of active sites on the surface of the material;  $1/y < 1$  implies multi-layer adsorption, whereas  $1/y > 1$  suggests that a given inhibitory molecule occupies more than one active site. Table 5 shows the parameters  $1/y$  found through the regression results for the inhibition efficiency calculated from weight loss (WL),  $R_p$  (PP) and EIS measurements. Here, it can be observed that, for weight loss, the values of the adsorption constant increase as the temperature increases, as indicated by the increase in efficiency (Table 1), and values greater than one of  $1/y$  indicate that adsorption occurs on more than one active site. For the other two experimental methods (polarization curves and EIS), the adsorption constant decreases and a multilayer adsorption begins to be observed. It is necessary to remember that, according to our studies, weight loss required 48 h of exposure of the sample, while the other experiments were performed after 30 min of conditioning of the metal in the corrosive medium. In agreement with Deng et al. [44], we observed that the effectiveness of inhibition depends on the immersion time.

**Table 5.** Parameters estimates derived through regression according to the isotherm of El-Awady.

	T (K)	$K_{ads}$ (L g <sup>-1</sup> )	$\Delta G^{\circ}_{ads}$ (kJ mol <sup>-1</sup> )	R <sup>2</sup>	1/y
WL	298	7.98	−22.25	0.99	4.22
	308	6.74	−22.56	0.96	2.09
	315	15.65	−24.72	0.97	1.61
	323	13.00	−24.24	0.99	1.33
PP	298	9.45	−22.67	0.73	1.27
	308	7.63	−22.88	0.94	0.87
	315	7.71	−23.43	0.77	0.19
	323	6.12	−23.40	0.95	0.37
EIS	298	10.60	−22.95	0.89	1.86
	308	5.45	−22.02	0.97	1.17
	315	5.20	−22.40	0.77	0.24
	323	4.11	−22.34	0.97	0.47

The changes in the standard free energy of adsorption were calculated through Equation (17):

$$\Delta G_{\text{ads}}^{\circ} = -RT \ln(C_{\text{H}_2\text{O}} \times K_{\text{ads}}) \quad (17)$$

where  $R$  is the gas constant,  $T$  is the absolute temperature, and  $C_{\text{H}_2\text{O}}$  is the concentration of water ( $1000 \text{ g L}^{-1}$ ) [33].

The sign of  $\Delta G_{\text{ads}}^{\circ}$  indicates that this is a spontaneous phenomenon and its value gives an idea of the type of behavior. Generally, values greater than  $-20 \text{ kJ mol}^{-1}$  are associated with electrostatic interactions between the surface of the metal and organic molecules, for example physical adsorption; values lower than  $-40 \text{ kJ mol}^{-1}$  indicate chemical adsorption; and values of about  $-22 \text{ kJ mol}^{-1}$  would indicate a mixed process involving both physical and chemical adsorption [48] or closer to physisorption [44].

To determine the change in the standard adsorption enthalpy  $\Delta H_{\text{ads}}^{\circ}$  and the standard entropy change  $\Delta S_{\text{ads}}^{\circ}$ , we used Equation (18):

$$\Delta G_{\text{ads}}^{\circ} = \Delta H_{\text{ads}}^{\circ} - T\Delta S_{\text{ads}}^{\circ} \quad (18)$$

and from the values of  $\Delta G_{\text{ads}}^{\circ}$  vs.  $T$ , we obtained the corresponding values of  $\Delta H_{\text{ads}}^{\circ}$  and  $\Delta S_{\text{ads}}^{\circ}$  based on weight loss experiments, where the value of  $\Delta H_{\text{ads}}^{\circ}$  results positive ( $6.81 \text{ kJ mol}^{-1}$ ), thus indicating that it is an endothermic process. Therefore, the increase in temperature favors the adsorption process. The value obtained for  $\Delta S_{\text{ads}}^{\circ}$  was positive and equal to  $97.3 \text{ J mol}^{-1} \text{ K}^{-1}$ , probably because during adsorption a quasi-substitution between the organic compounds and the water molecules takes place on the surface of the electrode. Then, the adsorption of organic molecules, which generates a decrease in entropy, is accompanied by desorption of water molecules, which generates an increase in entropy. Therefore, here, the entropy value is attributed to an increased entropy of solvents [49], which may be the driving force for the adsorption of inhibitors on the aluminum surface [50–53].

To distinguish between chemical and physical adsorption, we apply the Dubinin–Radushkevich isotherm [54], through Equation (19):

$$\ln \theta = \ln \theta_{\text{max}} - a\delta^2 \quad (19)$$

where  $\theta_{\text{max}}$  is the maximum surface coverage and  $\delta$  is the Polanyi potential, which is given by Equation (20)

$$\delta = RT \ln \left( 1 + \frac{1}{C_{\text{inh}}} \right) \quad (20)$$

where  $R$  is the gas constant,  $T$  is the absolute temperature, and  $C_{\text{inh}}$  is the concentration of the inhibitor expressed in  $\text{g L}^{-1}$ . A plot of  $\ln \theta$  vs.  $\delta^2$ , yields parameter  $a$ , whose value leads to the average adsorption energy,  $E_m$ , at the corresponding temperature.

This energy is required to transfer 1 mol of adsorbate from the bulk of the solution to the surface of the adsorbent, and is defined as:

$$E_m = \frac{1}{\sqrt{2a}} \quad (21)$$

When  $E_m < 8 \text{ kJ mol}^{-1}$  physical adsorption prevails, whereas if  $E_m > 8 \text{ kJ mol}^{-1}$  chemical adsorption dominates [48]. The values of  $E_m$  obtained here were  $10.10 \text{ kJ mol}^{-1}$  at 298 K,  $7.33 \text{ kJ mol}^{-1}$  at 308 K and 315 K and  $6.80 \text{ kJ mol}^{-1}$  at 323 K. This suggests that, as temperature increases, adsorption changes from chemical to physical, for weight loss data (Figure 7). However, according to impedance results, we obtained values lower than  $6.26 \text{ kJ mol}^{-1}$ , i.e., associated with physisorption for all temperatures.

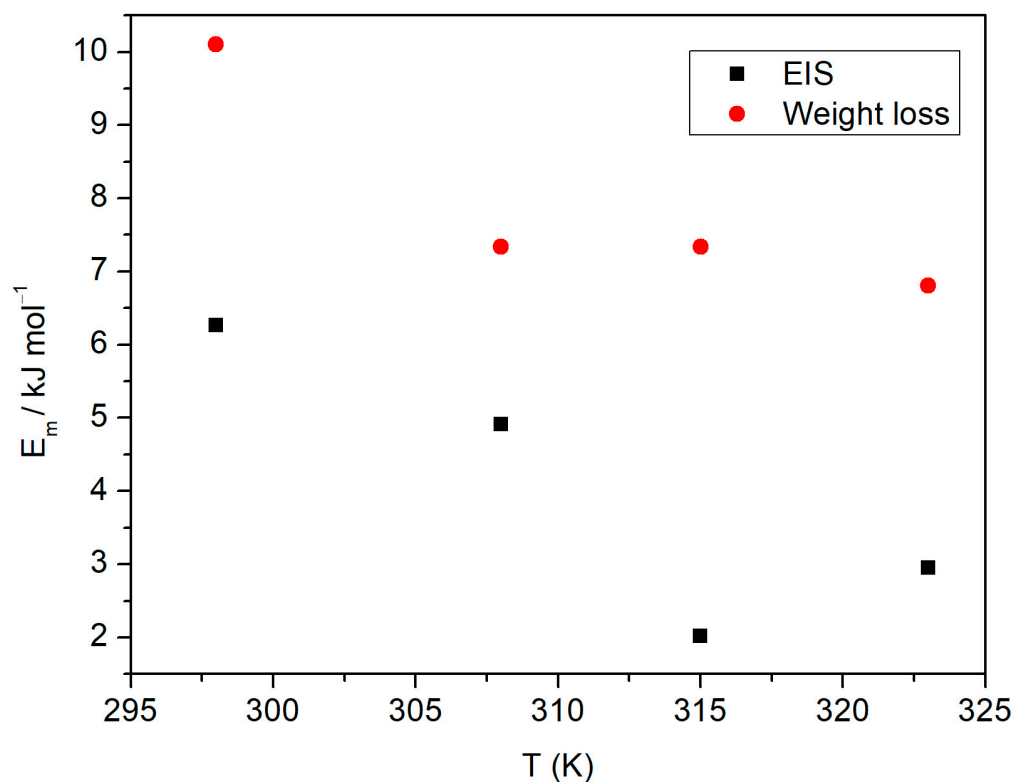


**Figure 7.** Adsorption energy vs. temperature of *Ilex paraguariensis* on aluminum.

In this work, the efficiency of *Ilex paraguariensis* as a corrosion inhibitor increased with temperature. In principle, this might be related to a chemisorption process, but the obtained free energy of adsorption may indicate the occurrence of physisorption. This discrepancy could be attributed to the fact that the application of adsorption isotherms for the analysis of inhibition phenomena and related data has many limitations. In addition, adsorption may be highly selective about the electrode reaction and may depend on the potential, while adsorbates compete with water molecules [55].

According to Souza et al. [34], the concentration of phenolic compounds in *Ilex paraguariensis* is higher than that in coffee, for the same amount of sample weighed to obtain both extracts, but the inhibition efficiency of *Ilex paraguariensis* is lower than that of coffee, so the inhibition effect may not be essentially caused by phenolic compounds.

### 3.6. Surface Analysis

The micrographs in Figure 8 show the surface of the aluminum before and after immersion in the corrosive solutions. Figure 8a shows the sample before immersion in 0.1 M HCl, where the surface exhibits some polishing grooves and scratches, whereas Figure 8b shows the sample after 48 h of immersion in the blank solution at 308 K, where the surface exhibits no inhibition and the presence of some degree of pitting. However, in the sample exposed to the maximum tested concentration of *Ilex paraguariensis*, at 308 K Figure 8c, the surface suffered less attack and there is no evidence of pitting, so it can be acknowledged that adsorption can efficiently retard the corrosion of aluminum. The same comparative morphological features between inhibited and blank conditions is observed in the whole studied T range, for example, the micrographs obtained at  $T = 323$  K, Figure 8d,e, are additionally presented since they relate to a singular mechanistic condition.

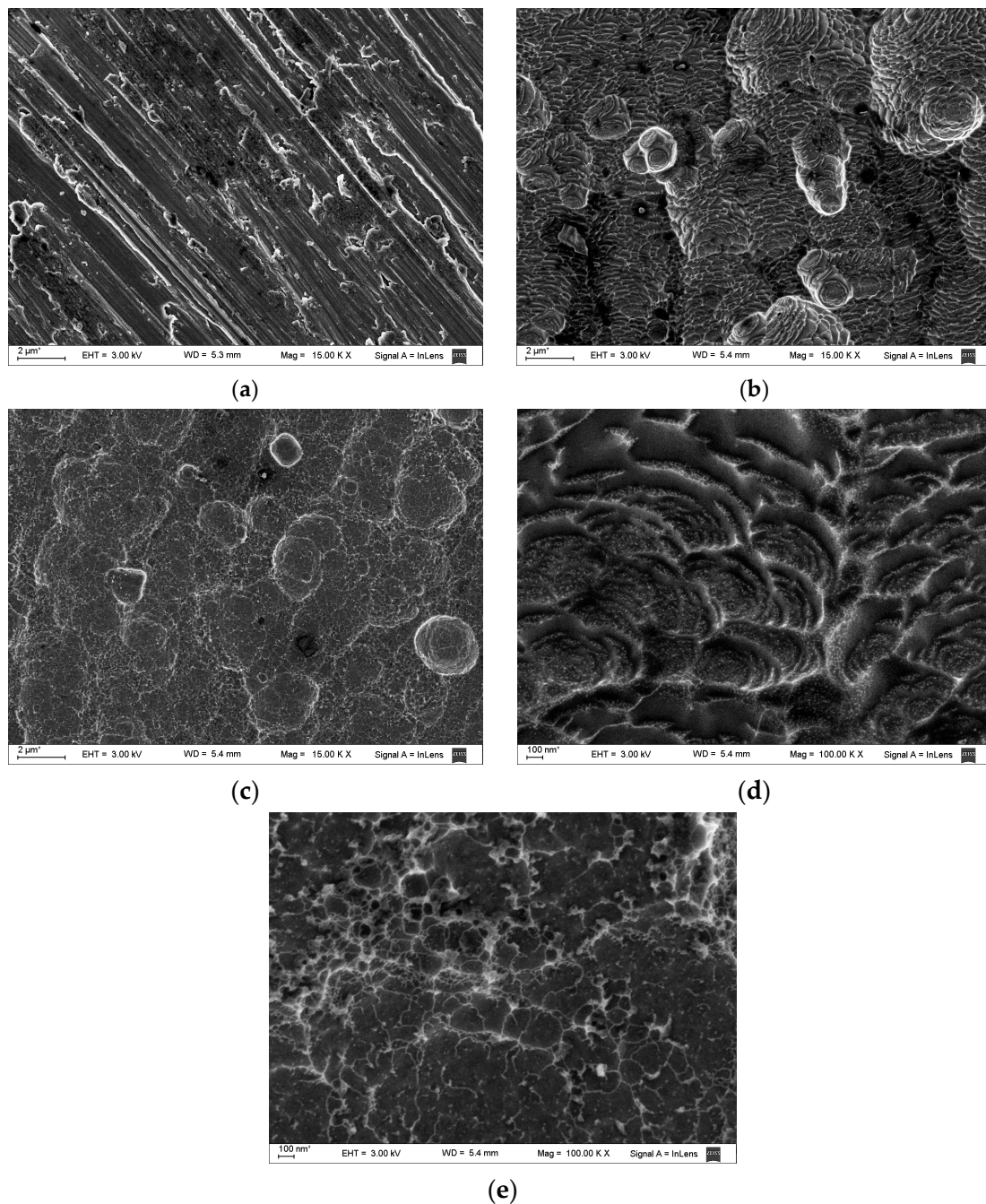


**Figure 8.** SEM images for (a) unexposed aluminum; (b) aluminum exposed to 0.1 M HCl without inhibitor and (c) aluminum exposed to 0.1 M HCl containing  $0.248 \text{ g L}^{-1}$  of *Ilex paraguariensis*, after 48 h of immersion at 308 K; (d) aluminum exposed to 0.1 M HCl without inhibitor and (e) aluminum exposed to 0.1 M HCl containing  $0.248 \text{ g L}^{-1}$  of *Ilex paraguariensis*, after 48 h of immersion at 323 K.

#### 4. Conclusions

1. *Ilex paraguariensis* is a good corrosion inhibitor for aluminum in 0.1 M HCl solution. The inhibition efficiency increases with its concentration, and, after 48 h exposure to the corrosive solution, efficiency increases with temperature. Maximum efficiency values (69 and 71%) were achieved at a concentration of  $0.248 \text{ g L}^{-1}$  of *Ilex paraguariensis* at 315 K and 323 K, respectively.
2. The adsorption of *Ilex paraguariensis* occurs in agreement with the isotherm of El-Awady that considers the phenomenon of adsorption by active sites. The process of adsorption is endothermic, and is accompanied by an increase in entropy.

3. An increase in the concentration of *Ilex paraguariensis* improves its performance as an inhibitor.
4. *Ilex paraguariensis* acts as a mixed-type inhibitor.
5. Complex EIS results were successfully understood in terms of a theoretical model of the interface where adsorption by the inhibitor's molecules hinders the progress of the electrochemical reactions related to the corrosive attack.

**Supplementary Materials:** The following supporting information can be downloaded at: <https://www.mdpi.com/article/10.3390/coatings13020434/s1>, Figure S1. Nyquist and Bode representations of experimental data and fit results of electrode impedance recorded for the system Al/0.1 M HCl in the absence and in the presence of different concentrations of the inhibitor at 298 K (a) and (b), and 315 K (c) and (d).

**Author Contributions:** Conceptualization, C.M.M.; methodology, C.M.M.; formal analysis, C.M.M. and C.A.G.; investigation, C.M.M. and G.P.; resources, A.E.A.; data curation, C.M.M. and C.A.G.; writing—original draft preparation, C.M.M. and C.A.G.; writing—review and editing, C.M.M., C.A.G. and A.E.A.; visualization, A.E.A.; supervision, A.E.A.; project administration, C.M.M.; funding acquisition, C.M.M. and A.E.A. All authors have read and agreed to the published version of the manuscript.

**Funding:** Consejo Nacional de Investigaciones Científicas y Técnicas (CONICET): RES.2019-574-APN-DIR#CONICET; Agencia Nacional de Promoción Científica y Tecnológica: PICT-2017-0079.

**Institutional Review Board Statement:** Not applicable.

**Informed Consent Statement:** Not applicable.

**Data Availability Statement:** The data presented in this study are available on reasonable request.

**Acknowledgments:** C.M.M. and G.P. appreciate the support provided by the Universidad Nacional de Misiones. C.A. Gervasi explicitly acknowledges the Buenos Aires Commission for Scientific and Technological Research (CICBA) as a senior research member of this Institution. A.E.A. gratefully thanks the National Scientific CONICET (Consejo Nacional de Investigaciones Científicas y Técnicas).

**Conflicts of Interest:** The authors declare no conflict of interest.

## References

1. Bentiss, F.; Traisnel, M.; Lagrenee, M. The substituted 1,3,4-oxadiazoles: A new class of corrosion inhibitors of mild steel in acidic media. *Corros. Sci.* **2000**, *42*, 127–146. [[CrossRef](#)]
2. Noor, E.A. The inhibition of mild steel corrosion in phosphoric acid solutions by some N-heterocyclic compounds in the salt form. *Corros. Sci.* **2005**, *47*, 33–55. [[CrossRef](#)]
3. Lagrenee, M.; Mernari, B.; Chaibi, N.; Traisnel, M.; Vezin, H.; Bentiss, F. Investigation of the inhibitive effect of substituted oxadiazoles on the corrosion of mild steel in Cl medium. *Corros. Sci.* **2001**, *43*, 51–962. [[CrossRef](#)]
4. Bethencourt, M.; Botana, F.J.; Calvino, J.J.; Marcos, M.; Rodriguez-Chacon, M.A. Lanthanide compounds as environmentally friendly corrosion inhibitors of aluminium alloys—A review. *Corros. Sci.* **1998**, *39*, 1803–1819. [[CrossRef](#)]
5. Arenas, M.A.; Conde, A.; de Damborenea, J. Cerium: A suitable green corrosion inhibitor for tinplate. *Corros. Sci.* **2002**, *44*, 511–520. [[CrossRef](#)]
6. Cano, E.; Pinilla, P.; Polo, J.L.; Bastidas, J.M. Copper corrosion inhibition by fast green, fuchsin acid and basic compounds in citric acid solution. *Mater. Corros.* **2003**, *54*, 222–228. [[CrossRef](#)]
7. Montemor, M.F. Fostering green inhibitors for corrosion prevention. In *Active Protective Coatings*; Series in Materials Science; Hughes, A., Mol, J., Zheludkevich, M., Buchheit, R., Eds.; Springer: Dordrecht, The Netherlands, 2016; Volume 233, pp. 107–137.
8. Sharmin, E.; Ahmad, S.; Zafar, F.; Islamia, J.M. *Corrosion Resistance*, 1st ed.; InTech: Rijeka, Croatia, 2012; pp. 449–472.
9. Moretti, G.; Guidi, F.; Grion, G. Tryptamine as a green iron corrosion inhibitor in 0.5 M deaerated sulphuric acid. *Corros. Sci.* **2004**, *46*, 387–403. [[CrossRef](#)]
10. de Souza, F.S.; Giacomelli, C.; Gonçalves, R.S.; Spinelli, A. Adsorption behavior of caffeine as a green corrosion inhibitor for copper. *Mater. Sci. Eng.* **2012**, *C 32*, 2436–2444. [[CrossRef](#)]
11. Raja, P.B.; Sethuraman, M.G. Natural products as corrosion inhibitor for metals in corrosive media—A review. *Mater. Lett.* **2008**, *62*, 113–116. [[CrossRef](#)]
12. Sharma, S.K.; Mudhoo, A.; Khamis, E.; Jain, G. Green Corrosion Inhibitors: An Overview of Recent Research. *J. Corros. Sci. Eng.* **2008**, *11*, 14. Available online: [https://www.researchgate.net/publication/285599848\\_Green\\_Corrosion\\_Inhibitors\\_An\\_Overview\\_of\\_Recent\\_Research](https://www.researchgate.net/publication/285599848_Green_Corrosion_Inhibitors_An_Overview_of_Recent_Research) (accessed on 5 January 2023).

13. Alvarez, P.E.; Fiori-Bimbi, M.V.; Neske, A.; Brandán, S.A.; Gervasi, C.A. Rollinia occidentalis extract as green corrosion inhibitor for carbon steel in HCl solution. *J. Ind. Eng. Chem.* **2018**, *58*, 92–99. [[CrossRef](#)]
14. Casaletto, M.P.; Figà, V.; Privitera, A.; Bruno, M.; Napolitano, A.; Piacente, S. Inhibition of Cor-Ten steel corrosion by “green” extracts of Brassica campestris. *Corros. Sci.* **2018**, *136*, 91–105. [[CrossRef](#)]
15. Ji, G.; Anjum, S.; Sundaram, S.; Prakash, R. Musa paradisiaca peel extract as green corrosion inhibitor for mild steel in HCl solution. *Corros. Sci.* **2015**, *90*, 107–117. [[CrossRef](#)]
16. Kumar, D.; Jain, V.; Rai, B. Unravelling the mechanisms of corrosion inhibition of iron by henna extract: A density functional theory study. *Corros. Sci.* **2018**, *142*, 102–109. [[CrossRef](#)]
17. Ennouri, A.; Essahli, M.; Lamiri, A. Corrosion Inhibition of Aluminum in Hydrochloric Acid Medium by Essential Oil of Eucalyptus camaldulensis and Myrtus Communis. *Anal. Bioanal. Electrochem.* **2019**, *11*, 913–929.
18. Loto, C.A.; Joseph, O.O.; Loto, R.T.; Popoola, A.P.I. Corrosion Inhibitive Behaviour of Camellia Sinensis on Aluminium Alloy in H<sub>2</sub>SO<sub>4</sub>. *Int. J. Electrochem. Sci.* **2014**, *9*, 1221–1231.
19. Ennouri, A.; Lamiri, A.; Essahli, M. Corrosion Inhibition of Aluminium in Acidic Media by Different Extracts of Trigonellafoenum-graecum L Seeds. *Port. Electrochim. Acta* **2017**, *35*, 279–295. [[CrossRef](#)]
20. Fares, M.M.; Maayta, A.K.; Al-Qudah, M.M. Pectin as promising green corrosion inhibitor of aluminum in hydrochloric acid solution Mohammad. *Corros. Sci.* **2012**, *60*, 112–117. [[CrossRef](#)]
21. Hechiche, N.; Boughrara, D.; Kadri, A.; Dahmani, N.; Benbrahim, N. Artemisia Herba Alba Essential Oil as Green Corrosion Inhibitor for Aluminum in Hydrochloric Acid Solution. *Anal. Bioanal. Electrochem.* **2019**, *11*, 1129–1147.
22. Nathiya, R.S.; Raj, V. Evaluation of Dryopteris cochleata leaf extracts as green inhibitor for corrosion of aluminium in 1 M H<sub>2</sub>SO<sub>4</sub>, Egypt. *J. Pet.* **2017**, *26*, 313–323.
23. Bashir, S.; Singh, G.; Kumar, A. Shatavari (Asparagus Racemosus) as Green Corrosion Inhibitor of Aluminium in Acidic Medium. *Port. Electrochim. Acta* **2019**, *37*, 83–91. [[CrossRef](#)]
24. Anbarasi, C.M.; Divya, G. A Green Approach to Corrosion Inhibition of Aluminium in Acid Medium Using Azwain Seed Extract. *Mater. Today Proc.* **2017**, *4*, 5190–5200. [[CrossRef](#)]
25. Obot, I.B.; Obi-Egbedi, N.O.; Umoren, S.A.; Ebenso, E.E. Synergistic and Antagonistic Effects of Anions and Ipomoea involucreta as Green Corrosion Inhibitor for Aluminium Dissolution in Acidic Medium. *Int. J. Electrochem. Sci.* **2010**, *5*, 994–1007.
26. Wisdom, J.; Kelechi, D.; Ugochukwu, J. Green Inhibitor for Corrosion of Aluminium Alloy AA8011A in Acidic Environment. *Int. Res. J. Eng. Technol.* **2018**, *5*, 121–124.
27. Khan, G.; Newaz, K.M.S.; Basirun, W.J.; Ali, H.B.M.; Faraj, F.L.; Khan, G.M. Application of Natural Product Extracts as Green Corrosion Inhibitors for Metals and Alloys in Acid Pickling Processes—A review. *Int. J. Electrochem. Sci.* **2015**, *10*, 6120–6134.
28. Berté, K.A.; Beux, M.R.; Spada, P.K.; Salvador, M.; Hoffmann-Ribani, R. Chemical Composition and Antioxidant Activity of Yerba-Mate (Ilex paraguariensis A.St.-Hil., Aquifoliaceae) Extract as Obtained by Spray Drying. *J. Agric. Food Chem.* **2011**, *59*, 5523–5527. [[CrossRef](#)] [[PubMed](#)]
29. Hartwig, V.G.; Ponce Cevallos, P.A.; Schmalko, M.E.; Brumovsky, L.A. Effects of Spray Drying Conditions on the Stability and Antioxidant Properties of Spray-Dried Soluble Mate. *Int. J. Food Eng.* **2014**, *10*, 131–138. [[CrossRef](#)]
30. Pomilio, A.B.; Trajtemberg, S.; Vitale, A.A. High-Performance Capillary Electrophoresis Analysis of mate infusions prepared from stems and leaves of Ilex paraguariensis using Automated Micellar Electrokinetic Capillary Chromatography. *Phytochem. Anal.* **2002**, *13*, 235–241. [[CrossRef](#)]
31. Heck, C.I.; Demejia, E.G. Yerba Mate Tea (Ilex paraguariensis): A Comprehensive Review on Chemistry, Health Implications, and Technological Considerations. *J. Food* **2007**, *72*, 138–151. [[CrossRef](#)]
32. Bockris, J.O.M.; Yang, B. The mechanism of corrosion inhibition of iron in acid solution by acetylenic alcohols. *J. Electrochem. Soc.* **1991**, *138*, 2237–2252. [[CrossRef](#)]
33. Mourya, P.; Banerjee, S.; Singh, M.M. Corrosion inhibition of mild steel in acidic solution by Tagetes erecta (Marigold flower) extract as a green inhibitor. *Corros. Sci.* **2014**, *85*, 352–363. [[CrossRef](#)]
34. Souza, T.F.; Magalhães, M.; Torres, V.V.; D’Elia, E. Inhibitory Action of Ilex paraguariensis Extracts on the Corrosion of Carbon Steel in HCl Solution. *Int. J. Electrochem. Sci.* **2015**, *10*, 22–33.
35. de Souza, F.S.; Spinelli, A. Caffeic acid as a green corrosion inhibitor for mild steel. *Corros. Sci.* **2009**, *51*, 642–649. [[CrossRef](#)]
36. Znini, M.; Majidi, L.; Bouyanzer, A.; Paolini, J.; Desjobert, J.M.; Costa, J.; Hammouti, B. Essential oil of Salvia aucheri mesatlantica as a green inhibitor for the corrosion of steel in 0.5 M H<sub>2</sub>SO<sub>4</sub>. *Arab. J. Chem.* **2012**, *5*, 467–474. [[CrossRef](#)]
37. Noor, E.A.; Al-Moubaraki, A.H. Thermodynamic study of metal corrosion and inhibitor adsorption processes in mild steel/1-methyl-4[4 (-X)-styryl pyridinium iodides/hydrochloric acid systems. *Mater. Chem. Phys.* **2008**, *110*, 145–154. [[CrossRef](#)]
38. Soltani, N.; Tavakkoli, N.; Khayatkashani, M.; Jalali, M.R.; Mosavizade, A. Green approach to corrosion inhibition of 304 stainless steel in hydrochloric acid solution by the extract of Salvia officinalis leaves. *Corros. Sci.* **2012**, *62*, 122–135. [[CrossRef](#)]
39. Hukovic-Metikos, M.; Babik, R.; Grubac, Z. The study of aluminium corrosion in acidic solution with nontoxic inhibitors. *J. Appl. Electrochem.* **2002**, *32*, 35–41. [[CrossRef](#)]
40. Abd El Haleem, S.M.; Abd El Wanees, S.; Abd El Aal, E.E.; Farouk, A. Factors affecting the corrosion behaviour of aluminium in acid solutions. I. Nitrogen and/or sulphur-containing organic compounds as corrosion inhibitors for Al in HCl solutions. *Corros. Sci.* **2013**, *68*, 1–13. [[CrossRef](#)]

41. Brett, C.M.A. The application of electrochemical impedance techniques to aluminium corrosion in acidic chloride solution. *J. Appl. Electrochem.* **1990**, *20*, 1000–1003. [[CrossRef](#)]
42. Epelboin, I.; Keddam, M.; Takenouti, H. Use of impedance measurements for the determination of the instant rate of metal corrosion. *J. Appl. Electrochem.* **1972**, *2*, 71–79. [[CrossRef](#)]
43. Itagaki, M.; Taya, A.; Imamura, M.; Saruwatari, R.; Watanabe, K. Interpretation of Faradaic Impedance for Corrosion Monitoring. *Corr. Sci. Technol.* **2004**, *3*, 1–5.
44. Deng, S.; Xianghong, L. Inhibition by Ginkgo leaves extract of the corrosion of steel in HCl and H<sub>2</sub>SO<sub>4</sub> solutions. *Corros. Sci.* **2012**, *55*, 407–415. [[CrossRef](#)]
45. Halambek, J.; Berković, K. Inhibitive Action of *Anethum graveolens* L. oil on Aluminium Corrosion in Acidic Media. *Int. J. Electrochem. Sci.* **2012**, *7*, 8356–8368.
46. Cardozo da Rocha, J.; da Cunha Ponciano Gomes, J.A.; D'Elia, E. Corrosion inhibition of carbon steel in hydrochloric acid solution by fruit peel aqueous extracts. *Corros. Sci.* **2010**, *52*, 2341–2348. [[CrossRef](#)]
47. Cao, C. On electrochemical techniques for interface inhibitor research. *Corros. Sci.* **1996**, *38*, 2073–2082. [[CrossRef](#)]
48. Amin, M.A.; El-Rehim, S.S.A.; El-Sherbini, E.E.F.; Bayoumi, R.S. The inhibition of low carbon steel corrosion in hydrochloric acid solutions by succinic acid. Part I. Weight loss, polarization, EIS, PZC, EDX and SEM studies. *Electrochim. Acta* **2007**, *52*, 3588–3600. [[CrossRef](#)]
49. Beda, R.H.B.; Niamien, P.M.; Avo Bilé, E.B.; Trokourey, A. Inhibition of Aluminium Corrosion in 1.0 M HCl by Caffeine: Experimental and DFT Studies. *Adv. Chem.* **2017**, *2017*, 6975248. [[CrossRef](#)]
50. Morad, M.S.; Sarhan, A.A.O. Application of some ferrocene derivatives in the field of corrosion inhibition. *Corros. Sci.* **2008**, *50*, 744–753. [[CrossRef](#)]
51. Villamil, R.F.V.; Corio, P.; Agostinho, S.M.L.; Rubim, J.C. Effect of sodiumdodecylsulfate on copper corrosion in sulfuric acid media in the absence and presence of benzotriazole. *J. Electroanal. Chem.* **1999**, *472*, 112–119. [[CrossRef](#)]
52. El-Awady, A.A.; Abd-El-Nabey, B.A.; Aziz, S.G. Kinetic-Thermodynamic and Adsorption Isotherms Analyses for the Inhibition of the Acid Corrosion of Steel by Cyclic and Open-Chain Amines. *J. Electrochem. Soc.* **1992**, *139*, 2149–2154. [[CrossRef](#)]
53. Deng, S.; Li, X. Inhibition by Jasminum nudiflorum Lindl. leaves extract of the corrosion of aluminium in HCl solution. *Corros. Sci.* **2012**, *64*, 253–262. [[CrossRef](#)]
54. Noor, E.A. Potential of aqueous extract of Hibiscus sabdariffa leaves for inhibiting the corrosion of aluminum in alkaline solutions. *J. Appl. Electrochem.* **2009**, *39*, 1465–1475. [[CrossRef](#)]
55. Umoren, S.A.; Eduok, U.M.; Israel, A.U.; Obot, I.B.; Solomon, M.M. Coconut coir dust extract: A novel eco-friendly corrosion inhibitor for Al in HCl solutions. *Green Chem. Lett. Rev.* **2012**, *5*, 303–313. [[CrossRef](#)]

**Disclaimer/Publisher's Note:** The statements, opinions and data contained in all publications are solely those of the individual author(s) and contributor(s) and not of MDPI and/or the editor(s). MDPI and/or the editor(s) disclaim responsibility for any injury to people or property resulting from any ideas, methods, instructions or products referred to in the content.